

# A Twin-CME Scenario for Ground Level Enhancement Events

G. Li · R. Moore · R.A. Mewaldt · L. Zhao ·  
A.W. Labrador

Received: 31 January 2011 / Accepted: 8 August 2011  
© Springer Science+Business Media B.V. 2011

**Abstract** Ground Level Enhancement (GLEs) events are extreme Solar Energetic Particle (SEP) events. Protons in these events often reach  $\sim$ GeV/nucleon. Understanding the underlying particle acceleration mechanism in these events is a major goal for Space Weather studies. In Solar Cycle 23, a total of 16 GLEs have been identified. Most of them have preceding CMEs and in-situ energetic particle observations show some of them are enhanced in ICME or flare-like material. Motivated by this observation, we discuss here a scenario in which two CMEs erupt in sequence during a short period of time from the same Active Region (AR) with a pseudo-streamer-like pre-eruption magnetic field configuration. The first CME is narrower and slower and the second CME is wider and faster. We show that the magnetic field configuration in our proposed scenario can lead to magnetic reconnection between the open and closed field lines that drape and enclose the first CME and its driven shock. The combined effect of the presence of the first shock and the existence of the open close reconnection is that when the second CME erupts and drives a second shock, one finds both an excess of seed population and an enhanced turbulence level at the front of the second shock than the case of a single CME-driven shock. Therefore, a more efficient particle acceleration will occur. The implications of our proposed scenario are discussed.

**Keywords** Solar energetic particles · Ground level enhancement events · Diffusive shock acceleration

---

G. Li (✉) · L. Zhao  
Department of Physics and CSPAR, University of Alabama in Huntsville, Huntsville, AL 35899, USA  
e-mail: [gang.li@uah.edu](mailto:gang.li@uah.edu)

R. Moore  
Space Science Office, VP62, Marshall Space Flight Center, Huntsville, AL 35812, USA

R.A. Mewaldt · A.W. Labrador  
SRL, Caltech 220-47 Downs, Pasadena, CA 91125, USA

## 1 Introduction

Understanding the acceleration and transport of Solar Energetic Particles (SEPs) in the inner heliosphere is one of the outstanding problems in heliospheric physics. Solar Energetic Particles pose major radiation hazards for spacecraft and astronauts. Particles over several hundred MeVs, when penetrating through the polar cap, can affect the health of airline crew and passengers on polar flights. The subsequent CME drivers also affect communication and navigation systems through induced geomagnetic storms.

Over the past several decades, a tremendous amount of data on SEPs has been obtained. It is now generally believed that the Sun accelerates particles to high energies mainly via two processes: solar flares and coronal mass ejections (CMEs). The observed temporal profiles of particles at 1 AU for these two processes are often different, with flare events being more “impulsive” and CME shock events being more “gradual” (Reames 1995, 1999), leading to the traditional categorization of “impulsive” SEP events and “gradual” SEP events. Besides the observed temporal profiles, spectra, abundances, and ionization states of energetic particles in these two classes also differ substantially (see e.g. recent surveys on CME-driven shocks and associated SEP events, (Desai et al. 2003, 2004; Ho et al. 2003), and surveys on ion composition and spectra during SEP events (Tylka et al. 1995, 2005; Cohen et al. 2003; Mewaldt et al. 2005, 2007).

One type of gradual SEP event is the Ground Level Enhancement events (GLEs). In these events, protons and ions are accelerated to very high energies (beyond  $\sim 500$  MeV/amu) with intensities often 10 to 100 times larger than normal gradual SEP events. At ground, these events have been observed since the 1940s by ionization chambers and neutron monitors. One intriguing question about GLEs is: what is different in a GLE event from a normal large SEP event? In particular, why are GLE events much stronger and larger than normal large SEP events?

In the last solar cycle (solar cycle 23), a total of 16 GLEs have been identified. In comparison, over a hundred SEP events have been recorded. While the number of GLE events is small, the observed particle time intensity profiles and spectra of GLEs are similar (although stronger and extended to higher energies) to those of normal SEP events. It is therefore natural to conjecture that GLE events share the same diffusive shock acceleration mechanism with the normal SEP events and the reasons that GLEs have larger intensity and higher energies are due to some fortuitous conditions that do not occur in most gradual SEP events.

Useful information about the acceleration sites in GLE and in general SEP events can be deduced from combining remote sensing observations of gamma rays, X-rays and radio signals and in-situ observations of energetic ions and electrons. Most of the gamma rays and hard X-rays are generated when energetic ions and electrons collide with the solar atmosphere. Recent RHESSI measurements (Shih et al. 2009) of the 2.223 MeV neutron-capture line (produced by  $>30$  MeV protons) and hard X-rays with energy  $>0.3$  MeV (produced by electron bremsstrahlung continuum emissions), for a total of 29 flare events, showed that these emissions are nicely correlated for flares of varying magnitudes. Therefore they provide timing information for energetic ions and electrons from solar flares (Lin et al. 2002).

Type II radio bursts have been often used as a diagnostic of the CME and its driven shock in studying SEP events (see e.g. Kahler 1982; Kahler et al. 2000; Cane et al. 2002; Cliver et al. 2004; Gopalswamy et al. 2005; Cho et al. 2008). Type II radio bursts are caused by shock-accelerated electrons radiating at local plasma frequencies. As the shock moves, the ambient plasma density falls and the radio burst drifts to lower frequencies. Type II radio bursts, according to their wave-length ranges, are classified as metric, decameter-hectometric (DH) and kilometric types respectively. Metric Type II radio bursts have a

frequency range of 150 to 15 MHz and are observed with ground based radio telescopes. DH (1–14 MHz) and kilometric ( $<1$  MHz) radio bursts are obtained via space-borne radio experiments. Metric type II radio bursts are generated when the shock is close to the Sun  $\leq 3R_{\odot}$  (Gopalswamy et al. 2009). While many SEP events have metric type II bursts associated with them, the observation of metric type II bursts do not necessarily lead to a “large” SEP event. Indeed, Kahler (1982), after examining a total of 58 metric events that occurred within W10–W85 from 1973 through 1980, found that only 31 were associated with 20 MeV SEP events. Later, Cliver et al. (2004) argued that the presence of the DH type (1–14 MHz) radio bursts may be used as a marker to distinguish between SEP-associated and non-SEP associated metric type II bursts. Using the WAVES experiment onboard the Wind Spacecraft, Cliver et al. (2004) showed that between 1996 July and 2001 June, 26 out of 29 of DH type radio bursts that occurred in the western hemisphere were associated with 20 MeV SEP events (with peak fluxes  $\geq 10^{-3}$  protons  $\text{cm}^{-2} \text{s}^{-1} \text{sr}^{-1} \text{MeV}^{-1}$  at 20 MeV).

In comparison, in the same period only 17 out of 69 metric-only (without DH counterpart) type II radio bursts were associated with 20 MeV SEP events. Since the plasma frequency at  $3R_{\odot}$  is  $\sim 14$  MHz, Cliver et al. (2004) suggested that (1) acceleration to high energies mostly occurs beyond  $3R_{\odot}$  and (2) shocks that survive beyond  $3R_{\odot}$  are more stronger and broader and therefore likely to intercept open field lines connecting to the Earth. Gopalswamy et al. (2005) also examined the role of the metric radio bursts and DH radio bursts in large SEP events. They found that CMEs tend to be more energetic if radio bursts appear in all three wavelength ranges (i.e. from m-to-km). In particular, CMEs associated with type II bursts confined to the metric domain were less energetic and were associated with smaller flares than CMEs associated with DH type II bursts (Gopalswamy et al. 2010a), agreeing with Cliver et al. (2004). Furthermore, by noting that the solar sources that had a small fraction of m-to-km type II bursts with SEPs were poorly connected to the Earth, Gopalswamy et al. (2005) also pointed out that the magnetic connectivity plays a role in observing SEP events. In both (Cliver et al. 2004) and (Gopalswamy et al. 2005), the metric type radio bursts were regarded as an integral part of a CME propagating out from the low corona. However, Reiner et al. (2001) have argued that the metric type II radio burst is caused by flare-associated coronal shock and therefore is a signature of flare, not CME-driven shock. In a recent paper, Cho et al. (2008) made use of low coronal observations from MLSO MK coronagraphs of type II associated CMEs and suggested that shocks at the CME front and/or at a CME-streamer interaction at CME flank are the two main mechanisms for generating type II bursts. While the origin of metric type radio bursts is not completely clear, here we take the same view as Cliver et al. (2004) and Gopalswamy et al. (2005) and regard the drifting from m-to-km wavelengths to reflect the progression of a CME-driven shock from low corona to the interplanetary space. A very good example showing the drift evolving smoothly from metric to DH was given in Cliver et al. (2004).

Unlike electromagnetic signals (X-rays and radio bursts), which travel directly from the Sun to the Earth, energetic ions and electrons propagate along the interplanetary magnetic field. Therefore, obtaining release times at the Sun for these particles suffers two uncertainties: (1) the magnetic field in any given event may differ significantly from the Parker spiral; (2) existence of interplanetary turbulence will lead to pitch angle scattering, therefore distorting the propagation profile. Nevertheless, by studying the velocity dispersion from ions of different energies, one can obtain, to a rather good accuracy, both the path length and the release time (see for example, Tylka et al. 2003).

Using Wind, ACE, IMP8, and data from neutron monitors, Tylka et al. (2003) have obtained the release time of energetic particles at the Sun for three GLE events and two other SEP events. Subsequent works on release times of energetic particles for all GLE events in

cycle 23 have been reported recently by Reames (2009) and Gopalswamy et al. (2010b). These studies showed that for all GLE events, the CMEs (and the corresponding shocks) are very close to the Sun ( $<4r_{\odot}$ ) when the initial energetic particles are released.

This poses a strong constraint on the acceleration time scale for a diffusive shock acceleration scenario. Indeed, consider a strong CME-shock as an example: if we assume a shock speed of 1500 km/s, then the shock travels  $1r_{\odot}$  in about 8.5 minutes. If the energetic particles are released when the shock is at  $4r_{\odot}$  and if the shock is formed around  $1.5r_{\odot}$ , as suggested in the work of Lin et al. (2006), then the acceleration time scale is as short as 20 minutes.

Not all CMEs lead to SEP events. Earlier work (Kahler 1996) has shown that the maximum energy and the intensity of SEPs are generally correlated with the shock speed. Later, Kahler et al. (2000), using IMP 8 observation, examined 17 proton events in the energy range of  $28 < E < 43$  MeV from CMEs having speeds in a narrow range of 650 km/s to 850 km/s, and found that the peak intensities in these events vary by four orders of magnitudes. Kahler et al. (2000) suggested that the role of ambient energetic particle intensity is another deciding factor for the generation of a large SEP event. Of course, a higher ambient energetic particle intensity at 1 AU does not necessarily mean a higher ambient energetic particle intensity near the Sun where the shock is the strongest and where the acceleration occurs. Nevertheless, Kahler et al. (2000) pointed out that the seed population is an important factor in generating a large SEP event.

In a later work of Gopalswamy et al. (2004), the correlation of large SEP events with the presence of preceding CMEs (within 24 hours of the primary CME) was examined. A total of 57 large SEP events that had intensity  $>10$  pfu at  $>10$  MeV between 1996–2002 were studied. Among these, 23 had preceding CMEs (within 24 hours from the same active region) and 20 did not have preceding CMEs. The other 14 are labeled as “other” and were not included in the correlation study. The analysis of Gopalswamy et al. (2004) found a strong correlation between high particle intensity events and the existence of preceding CMEs, as shown in Fig. 11(a) of Gopalswamy et al. (2004). They concluded that “higher SEP intensities result whenever a CME is preceded by another wide CME from the same source region and the correlation between the peak intensity and the CME speed is improved substantially”.

Stimulated by Gopalswamy et al. (2004), Li and Zank (2005) noted that it is possible that the preceding CME creates an excess of interplanetary turbulence which significantly enhances the scattering rate (and decreases the acceleration time scale) of particles at the shock driven by the second CME, leading to a more effective diffusive shock acceleration process. Li and Zank (2005) further estimated the acceleration time scale at the second shock and showed that if the wave (turbulence) intensity downstream of the first shock (which is the upstream of the 2nd shock) is enhanced by a factor of 10, then a factor of 32 increase for the maximum particle kinetic energy may be reached at the second shock. In the work of Li and Zank (2005), the authors also noted that the preceding shock can provide the needed seed population at the second shock through pre-acceleration. Clearly, this requires the first shock and the second shock to occur closely in time so that the accelerated particles from the first shock do not propagate away before the second shock runs through them. However, putting an exact upper limit of the time separation between the two shocks is hard—as we will discuss later, however, 24 hours may be too long.

In-situ compositional studies indicate that many GLE events and large SEP events may have originated from seed populations that are different from the solar wind. The ratios Mg/O, Si/O, Fe/O and Ne/O have been used to distinguish solar wind material from ICME material (see e.g. Ipavich et al. 1986; Zurbuchen et al. 2002; Richardson and Cane 2004).

Recently, Mewaldt et al. (2007), using 2-hour average data from ACE/SWICS, showed that the Fe/O ratio in ICME material (see Fig. 9 in their paper) increases significantly above the solar wind value. ICME material is also known to be highly ionized (e.g.,  $\langle Q_{\text{Fe}} \rangle \sim 16$ ; see Lepri et al. 2001). We have Fe ionic charge state data from 10 GLEs. We see  $\langle Q_{\text{Fe}} \rangle \geq 14$  in 7 events and  $\langle Q_{\text{Fe}} \rangle \sim 20$  in 5 events (Mewaldt et al. 2011). For 9 large non-GLE events, 6 events have  $\langle Q_{\text{Fe}} \rangle \geq 14$  and  $\langle Q_{\text{Fe}} \rangle \sim 20$  in 2 events (see also Labrador et al. 2005). So, while it is true that large events have an excess of highly ionized Fe, the mean value  $\langle Q_{\text{Fe}} \rangle$  for GLEs is only 1.1 sigma greater than the mean value for non-GLEs (Mewaldt et al. 2011), suggesting that GLEs and large SEP events should be treated similarly.

In this paper, we discuss a possible mechanism for generating GLEs via multiple CMEs. We first illustrate the mechanism using two cartoons showing the sequence of the two CME eruptions. We point out that for the proposed mechanism to work, preceding CMEs of smaller speeds are favored. They also need not to be wide. We next examine the existence of preceding CMEs for the 16 GLEs in solar cycle 23. We show that all of these have weaker and slower preceding CME(s) within 9 hours of the primary one. Unlike the work of Gopalswamy et al. (2004), whose selection criteria for the preceding CME includes a  $> 60^\circ$  angular width and a 24 hour window, in our proposal, no constraints on the angular width are imposed. We however, do require the preceding CMEs to occur within a shorter window than 24 hours. This period is taken to be 9 hours which is our estimate of the decay time of the enhanced turbulence level. Even though Gopalswamy et al. (2004) used a 24-hour time window, the preceding CMEs were found to occur within a window of  $\sim 11$  hours (see their Fig. 10a, similar to the value used here. We also examine the composition and charge states in selected GLE events. We do not consider the underlying acceleration mechanism except that we note that both diffusive shock acceleration and acceleration due to reconnection, which occurs mainly at flare sites, can be involved in our proposed scenario. Theoretical details of applying these acceleration mechanisms in GLE events can be found in Aschwanden (2011) for particle acceleration at flares and Li (2011) for diffusive shock acceleration. For an observational overview of GLE events, readers are referred to Gopalswamy et al. (2010b). Also see Moraal and McCracken (2011) for timing and comparison of selected GLE events and the time structure of individual GLEs; Mewaldt et al. (2011) for in-situ observations of energetic particles of the 16 GLEs, including comparisons of their elemental, isotopic and ionic charge-state composition, and their energy spectra. Finally Nitta et al. (2011) studied the properties and magnetic field connection of GLE-producing ARs.

## 2 A “Twin-CME” Scenario for Extreme SEP Events

In Li and Zank (2005), the acceleration time scale at the second shock is estimated with the assumption that due to the presence of the first shock the turbulence at the second shock front is 10 times stronger than the case of no preceding shock. An implicit assumption in Li and Zank (2005) is that the material in the downstream of the first shock can be later processed by the second shock. However, the first CME can prevent the second CME from producing a shock. If the second CME occurs right beneath the first CME and close in time, as it overtakes the fast-moving flux-rope/plasmoid driver of the first CME, it might not produce a shock. Numerical simulations (Wang et al. 2005) showed that complicated interactions between the two CMEs may occur and eventually they will merge into one large ejection. In this case, the second shock may not be generated.

Another implicit assumption of Li and Zank (2005) is that the strong turbulence downstream of the first shock will stay there long enough and does not dissipate significantly

before the second shock arrives. This may not be valid if the separation between the two CMEs is as long as 24 hours. Assuming the downstream turbulence is mainly in the form of Alfvén waves which are transmitted from the upstream of the first shock, one can estimate the decay time of the turbulence: suppose the shock starts from  $2r_{\odot}$  with an average opening angle of  $60^{\circ}$ . We know from the timing study (Reames 2009; Gopalswamy et al. 2010b) that the acceleration occurs below  $\sim 4r_{\odot}$ , therefore, the region between  $2r_{\odot}$  and  $4r_{\odot}$  must be strongly turbulent. The length scale of this region is  $L \sim 2r_{\odot}$ . Low frequency Alfvén waves in this region presumably interact through 3-wave interactions and damp into sound waves (assuming  $\beta \sim 1$ ). If we can describe Alfvén waves in this strong turbulent region as diffusive in nature, i. e., a wave reverses its propagation direction in a distance of the characteristic low frequency (large scale) Alfvén wave length  $\lambda$ , then the decay time can be estimated as  $\tau \sim \frac{L}{\lambda} \frac{L}{V_A}$ . As an order of magnitude estimate, taking  $V_A = 450$  km/s and  $\lambda \sim 0.20r_{\odot}$  (Zaqarashvili et al. 2006), which corresponds to a period of 5 minutes, we have  $\tau \sim 8.7$  hours. This is  $\sim 3$  times shorter than the 24 hours separation threshold used in Gopalswamy et al. (2004). In a recent study by Chen et al. (2011), the authors also noted that the distribution of the time separation between two consecutive CMEs from the same active region shows clearly two population: one peaks at  $< 9$  hour and one peaks at  $> 9$  hours.

Finally, the work of Li and Zank (2005) did not consider the magnetic field configuration before the eruption of the CMEs and did not consider the possibility of having the driver material of the first CME or the flare material that accompanies the first CME as the seed particles for acceleration at the second shock. These issues were discussed in Li and Mewaldt (2009), who considered a specific scenario for generating extreme SEP events. In this scenario, two CMEs go off closely in time and slightly offset laterally. By considering explicitly reconnection of field lines that enclose the first CME and that drape the second CME, Li and Mewaldt (2009) argued that the material inside the first CME's driver can be processed by the second CME, leading to an enhancement of heavy ions that are compositionally ICME-like or flare-like. The work of Li and Mewaldt (2009) is stimulated by the observation of enhanced Fe/O and Ne/O ratio in some of the GLE events (Mewaldt et al. 2009). While the idea of introducing magnetic field line reconnection to access CME-driver material or flare material by the second shock is interesting, Li and Mewaldt (2009) did not present a clear eruption sequence. Furthermore, as pointed out in Li and Mewaldt (2009), not all GLE events show significant enhancement of Fe/O and Ne/O from the solar wind value.

We consider here explicitly the magnetic polarity arrangement of the active region source of the two consecutive CMEs and the effect of interchange reconnection between the closed field lines of the first CME and the open field lines that drape the second CME. This scenario is shown by the cartoon in Fig. 1. We refer to this scenario as the “twin-CME” scenario.

First, to avoid having the second CME interact with the first in a complicated manner and not produce a second shock, we follow Li and Mewaldt (2009) and consider the second CME to be laterally offset from the first one. As shown in Fig. 1, if the second CME occurs temporally close to the first CME, but laterally offset from the first CME, then it will NOT plow directly into the first CME. Instead, it erupts along side of the first CME. As we explain below, interchange reconnection of the first CME can put a large seed population of pre-accelerated particles in the turbulent downstream behind the first CME's shock. These seed particles are then accelerated by the second CME's shock to produce an extreme SEP event, having ICME-like and/or flare-like element abundances.

The sequence for this “twin-CME” scenario is the following:

(a) The leftmost panel of Fig. 1 shows at time  $t_0$  the initial magnetic field configuration at the solar surface before the eruption of the first CME. On the solar surface, two neutral

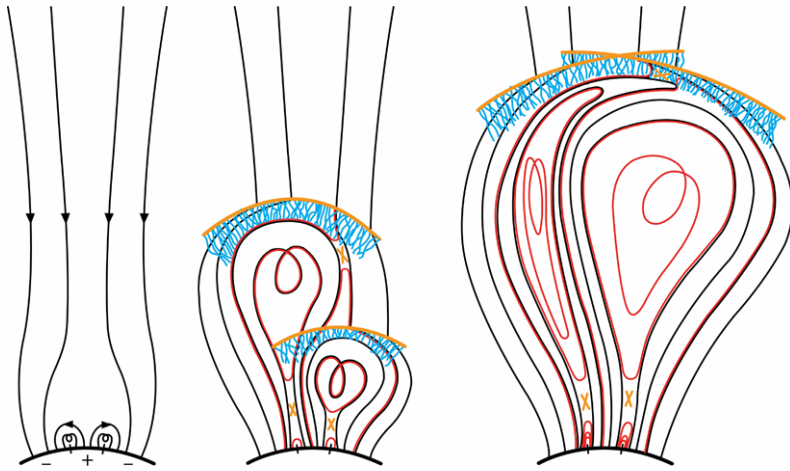


**Fig. 1** The cartoons depicting our “twin-CME” scenario for the generation of an extreme SEP event. Two CMEs erupt from the same or nearby source active regions. Interchange reconnection between open magnetic field and that enclosing the first CME can release driver material of the first CME to the turbulence-enhanced downstream of the first CME shock. This material can be subsequently accelerated by the second CME shock. See text for details

lines separate the magnetic field to  $-$ ,  $+$ , and  $-$  polarities. Far above the solar surface, the magnetic field is unipolar (shown as inward polarity). Note, even though the interplanetary current sheet (ICS) is much more convoluted during the maximum phase of the solar cycle than during the minimum phase, it always divides the inner heliosphere (out to  $\sim 0.3$  AU) into two tilted hemispheres with opposite polarity. Except during the passage of a CME, the half sphere on one side of the ICS is full of open magnetic field of one polarity and the other half full of open field of the opposite polarity.

(b) At a later time  $t_1$ , the first CME erupts and expands and drives a shock (the top orange curve in the second panel). Behind the shock is the turbulent downstream region. The strongest turbulent region is right behind the shock and is shown by the blue shaded area. Mostly likely this eruption occurs in one or the other of the two opposite-polarity open-field domains of the inner heliosphere. Hence, for nearly every CME, interchange reconnection can occur between the ambient open field and the opposite-polarity leg of the CME, as depicted for the first CME in Fig. 1. This reconnection can open the driver of the first CME and bring the “driver material” out of the closed plasmoid. The reconnection also accelerates some of the driver-material particles, although not to very high energies. Now if a second CME occurs on the side of the first CME where the interchange reconnection (shown as the top yellow cross) occurs, then the reconnection opens the driver of the first CME and releases the “driver material” into the turbulence-enhanced downstream of the first shock and upstream of the second shock. Note there are also reconnections and particle acceleration low down at the flare site (also marked by yellow crosses in Fig. 1). In our “twin CME” scenario, the interchange reconnection can also leak these flare particles into the turbulence enhanced upstream of the second shock.

(c) As the second shock plows through the turbulent plasma behind the first shock, it accelerates the pre-accelerated “driver material” or “flare material” seed particles provided by the interchange reconnection at the first CME. This acceleration is the most effective when the second shock is still close to the Sun. This is because the wave power (turbulence strength) downstream of the first shock decreases quickly with heliocentric distance (Zank

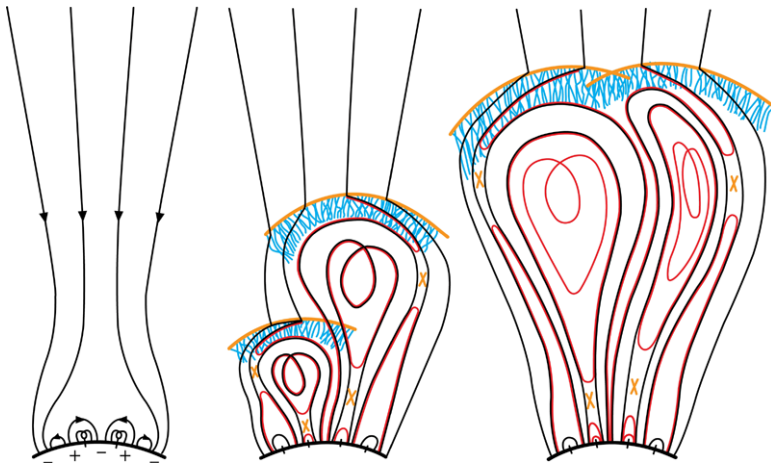


**Fig. 2** The cartoon showing the second CME and the inter-change reconnection between the open field line and that draping the first CME occurring on opposite sides of the first CME

et al. 2000; Li et al. 2003; Rice et al. 2003); therefore the acceleration to very high energies should occur close to the Sun. This is indeed what the timing studies (Tylka et al. 2003; Gopalswamy et al. 2010b, 2011; Reames 2009) suggested.

In Fig. 1 we assume the second shock catches up with the first shock. This is not necessary in the “twin CME” scenario. It can occur if the two CMEs erupt close in time and the second shock overtakes the first. However, this is not necessarily required for our scenario to produce a GLE. This can be seen from the following: again assuming both shocks start at  $2r_{\odot}$  then the second shock will catch up with the first at a height  $h$ ,

$$h = \frac{V_1 V_2}{V_2 - V_1} \Delta t \quad (1)$$

where  $V_1$  and  $V_2$  are the speeds of the first and the second shocks,  $\Delta t$  is the delay between them. Take  $V_1 = 800$  km/s,  $V_2 = 2000$  km/s, and  $\Delta t = 6$  hours, we have  $h = 42r_{\odot}$ . This is far beyond the inferred acceleration height of  $4r_{\odot}$  from the timing study. So, in our scenario the acceleration to high energy is purely due to diffusive shock acceleration at the second shock alone and does not require the interaction of the two shocks. Note if  $\Delta t$  becomes very short, say 30 minutes, then the interaction of the two shocks will occur below  $4r_{\odot}$  and it becomes important to consider particle acceleration at two converging shocks.

Besides the configuration shown in Fig. 1, it is possible to have the pre-eruption magnetic field as in Fig. 2. Here, the second CME and the inter-change reconnection between the open field and that enclosing the first CME occur on opposite sides of the first CME. Therefore, although the reconnection can bring the “driver material” or the “flare material” out of the plasmoid of the first CME, they are less likely to be processed by the second shock. One consequence of the “twin CME” scenario is that in cases described by Fig. 1 the composition of energetic particles would have signatures of ICME or flare material. This is not true for cases described by Fig. 2. In this case, the second shock still plows into the strong turbulence downstream of the first shock and is capable of producing a large SEP event or GLE event, but the composition of energetic particles will likely be more solar wind like.

To identify observed source-region field arrangements that match the scenarios shown in Figs. 1 and 2, it is important that we can unambiguously identify (1) the magnetic polarity

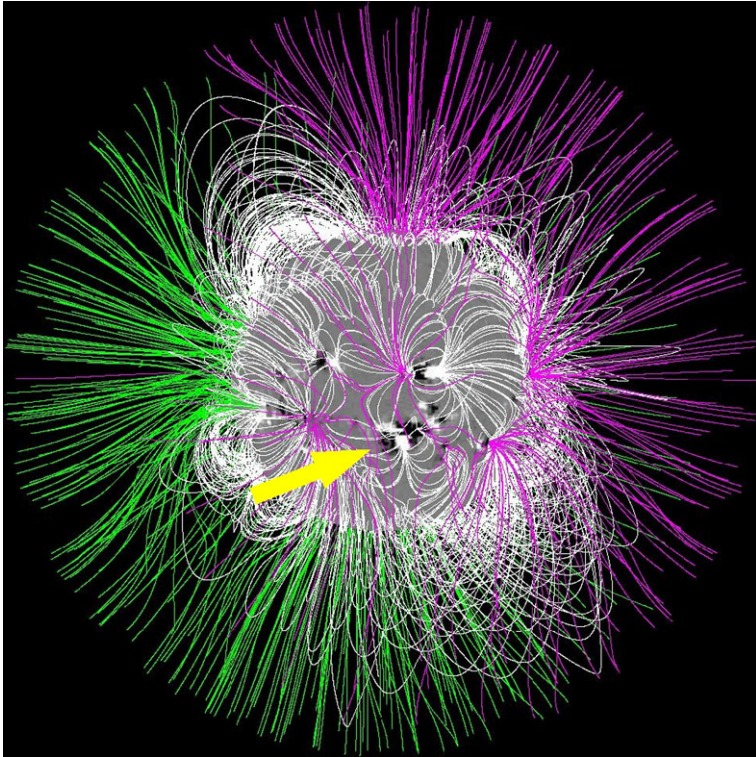


**Fig. 3** The potential Field Source Surface (PFSS) model global magnetic field computed for the Sun of the day of the 2003 Oct 28 GLE event. Courtesy of Dr. M. DeRosa at Lockheed Martin Solar and Astrophysics Laboratory. The arrow in the figure points to the source active region of the GLE's CME. In this case, the source active region is under the negative-polarity (*purple*) domain of the open field in the outer coronal and inner heliosphere. The polarity arrangement of the GLE source active region of 2003 Oct 28 is that of the Cartoon shown in Fig. 1

of the unipolar open field and the orientation of the closed field enclosing the driver of the first CME; and (2) the source active region(s) of the two consecutive CMEs, each source active region being identified by the flare it produces along with its CME.

We note that the cartoon field configurations in Figs. 1 and 2 are not meant to be realistic except to portray (1) the gross polarity arrangement of the magnetic field in the active region from which the two CMEs erupt, and (2) the polarity (direction) of the open field that fills the half of the heliosphere (the half on one side of the interplanetary current sheet) that the active region sits under, which field is rooted at widely distributed places outside the active region, none of which are necessarily as near to the active region as depicted in Figs. 1 and 2. An example of an actual GLE-producing active region that had the field arrangement drawn in Fig. 1 is AR10486, which produced the GLEs of 2003 October 28 and 29 (see the computed PFSS global field (Schrijver and DeRosa 2003) shown in Fig. 3). This active region had strong mostly positive flux sandwiched between strong mostly negative flux and the active region was located under the negative polarity domain of the heliosphere, as can be seen from Fig. 3, and also by comparing the synoptic map of the MDI photospheric magnetic flux for Carrington Rotation 2099 with the WSO synoptic map of the coronal source surface field computed for the source surface at  $3.25R_{\odot}$ . An example of an actual

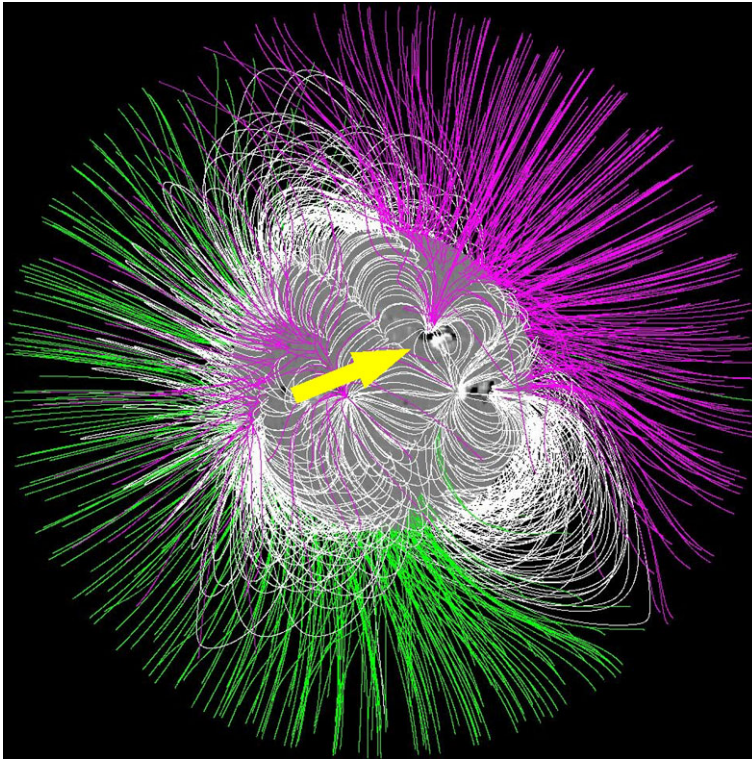


**Fig. 4** Similar to Fig. 3, but for the day of the 2005 Jan 17 GLE event. The polarity arrangement of the GLE source active region of 2005 Jan 17 is that of the Cartoon shown in Fig. 2

GLE-producing active region that had the field arrangement as drawn in Fig. 2 is AR10720 which produced the GLEs of 2005 January 17 and 20 (see Fig. 4). This active region had strong mostly negative flux sandwiched between strong mostly positive flux and sat on the negative-polarity side of the interplanetary current sheet according to the WSO synoptic map for Carrington Rotation 2025 computed for the source surface at  $3.25R_{\odot}$ .

Previous works on the effect of the initial magnetic polarity on the evolution of CME shocks has been investigated numerically by Chane et al. (2005), where plasmoids having the same and opposite senses from the background magnetic fields were considered. Our scenarios shown in Figs. 1 and 2 have some similarities to these cases. Recurrence of flare/CME events within a short period of time has been noted by Nitta and Hudson (2001) observationally. Lugaz et al. (2007a), in studying the 2000 November 24 event, also modeled multiple ejections from a single active region and obtained a complicated CME profile.

### 3 Preceding CMEs in GLE Events

In our twin-CME scenario, the role of the first CME is to provide the required seed particles through the open-closed reconnection and drives a shock to set up turbulence stronger than that in the solar wind in the front of the second CME shock.

In the standard diffusive shock acceleration (DSA) mechanism (Axford 1981; Drury 1983; Zank et al. 2000), the maximum particle energy is achieved by equating the accel-

eration time scale, given by,

$$t_{\text{acc}} = \int_{p_1}^{p_{\text{max}}} \beta \frac{\kappa(p)}{u_{sh}^2} \frac{dp}{p}, \quad (2)$$

where

$$\kappa = \kappa_{up}(p) + s\kappa_{dn}(p). \quad (3)$$

is the particle's diffusion coefficient and  $\beta = 3s/(s - 1)$  with  $s$  the shock compression ratio,  $p_1$  the particle injection momentum; to that of the shock dynamic scale (see, e. g. Li (2011)),

$$t_{\text{dyn}} = \min \left\{ \frac{R(t)}{dR(t)/dt}, \frac{B(t)}{dB(t)/dt}, \frac{n(t)}{dn(t)/dt} \right\}. \quad (4)$$

So the maximum momentum (energy) can be obtained through,

$$t_{\text{dyn}} = \int_{p_1}^{p_{\text{max}}} \beta \frac{\kappa}{u_{sh}^2} \frac{1}{p} dp. \quad (5)$$

The smaller the diffusion coefficient, the larger the maximum energy. At an oblique shock front, the value of  $\kappa$  is decided by the upstream turbulence level, which is proportional to the number density of injected particles. Therefore, both an increase of seed population and an enhanced turbulence level at the second shock will help to produce a smaller  $\kappa$ . Assuming the maximum particle energy at a single shock, with no enhance turbulence nor enhanced seed population, is 10 MeV/nuc; assuming the seed population is increased by a factor of 5 and the turbulence level due to being the downstream of the first shock increases by a factor of 10, then using (5) and assuming  $\kappa \sim p^\alpha$ , we find that the maximum particle energy at the second shock can reach  $\sim 1$  GeV for a typical value of  $\alpha$  being 1.5 or 2.0.<sup>1</sup>

The first shock need not be fast nor wide to drive a strong shock.<sup>2</sup> The only requirement for the speed is that the CME must be fast enough to drive a shock. Note, the Alfvén speed  $V_A$ , in some coronal models (Gopalswamy et al. 2001), as a function of height, has a local maximum at  $\sim 3R_\odot$ , therefore, depending on the CME speed, it may drive a shock close to the Sun and then unshock when the Alfvén speed increases and “shock” again. For our proposed scenario to work, the existence of the initial shock phase would be enough. In Gopalswamy et al. (2004), large SEP events are grouped according to the existence of preceding CMEs.

Gopalswamy et al. (2004) used the following three criteria for the preceding CME: (1) the preceding CME originated from the SAME source active region as the primary CME; (2) the preceding CMEs should have been launched within 24 hours ahead of the onset time of the primary CMEs, and (3) the preceding CMEs are wider than  $60^\circ$ . As discussed above, these criteria are not necessary for our proposed scenario. Instead our criteria are the following: (a) the preceding CME has to have a projected speed  $> 300$  km/s so that a shock can form; (b) the preceding CME has to be within 9 hours of the primary CME so that the strong turbulence downstream of the first shock did not decay away when the second shock plow through; (c) we impose no requirement of the width of the first CME, but the centerline of

---

<sup>1</sup>An  $\alpha$  value of 1.5 (2.0) corresponds to a shock compression ratio of 3.0 (2.5)

<sup>2</sup>The width of the preceding CME is less important than the width of the main CME. What is important in the scenario is for the shock driven by the second CME to plow into the downstream of the shock driven by the first CME. For that to occur the more aligned the propagation directions of the two CMEs, the better.

the first CME must be within the span of the second CME (i.e. the downstream of the first CME-driven shock should be plowed through by the second CME). We have examined all GLEs in the solar cycle 23 to see if these criteria are met. Note our choice of 300 km/s as the threshold of the projection speed depends on the knowledge of the Alfvén wave speed profile between 1 to 5 solar radii. Different models have been proposed in the literature (see Evans et al. 2008 and references therein). However, they do vary much. In Fig. 1(c) of Evans et al. (2008),  $V_A$ s from 8 model calculations in active regions have been plotted. Above  $2R_\odot$  and below  $3R_\odot$ , all models except one (*M7*) yield a  $V_A$  smaller than 300 km/s. The one (*M7*) that has a  $V_A > 300$  km/s gives a  $V_A \sim 500$  km/s around  $2R_\odot$  and has a maximum of 700 km/s at  $3.5R_\odot$ . Since the speeds of the CMEs are sky projection speeds, the physical speeds are larger (if the real propagation has a  $45^\circ$  with the plane of the sky, then the physical speed is  $\sim 450$  km/s), therefore our choice of the threshold speed of 300 km/s is reasonable.

In Table 1, we list our findings for all 16 GLE events during solar cycle 23. In identifying the preceding CMEs, we mainly made use of the online catalogs including the Coordinated Data Analysis Workshop (CDAW) Data Center catalog at [http://cdaw.gsfc.nasa.gov/CME\\_list/](http://cdaw.gsfc.nasa.gov/CME_list/); the Solar Eruptive Event Detection System (SEEDS) catalog at <http://spaceweather.gmu.edu/seeds/>; and the Computer Aided CME Tracking (CACTUS) catalog at <http://sidc.oma.be/cactus/>. We also made use of the Automatic Recognition of Transient Events and Marseille Inventory from Synoptic maps (ARTEMIS) catalog at <http://www.oamp.fr/lasco/> and the Naval Research Lab (NRL) catalog at <http://lasco-www.nrl.navy.mil/index.php?p=content/cmelist>. The flares that are associated with the preceding CMEs are obtained from the online Solar Geophysical Data database at <http://solarmonitor.org>.

The 1998 August 24 event has no LASCO data as SOHO was temporarily disabled at that time. We therefore did not analyze this event in this work. In Table 1, the first column is the GLE number and date. The preceding CMEs (and for the 1998 May 6 case, a trailing CME) for all GLEs are labeled by “-”. The second column is the Active region number and its location. The third column is the soft X-ray flare class and its onset time for the flares that are associated with the CMEs obtained from the Solar Geophysical Data database. The fourth column is the CME onset time as reported by the various catalogs. For all preceding CMEs we have tried to identify corresponding flares. As a criterium, we require the onset times of the flares as shown in column 3 to be within 70 minutes of the CME times shown in the column 4 (except for the 2000 July 14 event where a *C7.1* flare at 6:52 UT is identified to be associated with the 8:30 UT preceding CME. The background of the EIT image of the 2000 July 14 however, was too strong and there could be other flarings from the same active region between 6:52 UT and 8:30 UT). The fifth column is the CME sky-plane speed as given by the various catalogs. The sixth column is the Central Position Angle of the CME eruption as given by the various catalogs. The CPA is measured counter-clockwise from Solar North in degrees. The seventh column is the angular width of the CME as given by the various catalogs. The eighth column is the source of the database. While almost all GLEs are associated with halo CMEs, we do examine the LASCO movies for each event to ensure that the preceding CMEs and the primary CME, when projected to the plane of the sky, do overlap. From the 9th to the 12th columns, the ratio of Ne/O, Si/O, Mg/O and Fe/O at 12–30 MeV/nucleon for the GLE events are shown. In-situ data from ACE/SIS in-situ measurements are used in this analysis.

The SEEDS catalog made use of difference images and identified the most number of CMEs. Many of these are narrow flows and did not get picked out by other catalogs. They may be classified as jets. However, if the speeds of these jets exceed the Alfvén speed, we expect a shock to form although it may last only a short period of time. Note, for the

**Table 1** Properties of CMEs in GLE events of solar cycle 23

GLE number/date	AR number/loc	FC/onset time <sup>a</sup>	CME time	$\Delta r^b$	CME speed	CPA	AW	Database	Ne/O	Mg/O	Si/O	Fe/O
-	8100	C1.9/3:12	04:20	8	307	263	59	CDAW	-	-	-	-
55/1997.11.6	8100/S18W63	X9.4/11:49	12:10	-	1556	Halo	360	CDAW	0.26	0.202	0.169	0.650
-	8210	C5.4/4:48	05:31	8.5	352	228	80	SEEDS	-	-	-	-
56/1998.5.2	8210/S15W15	X1.1/13:31	14:06	-	958	298	91	CDAW	0.33	0.298	0.203	0.636
-	8210	M2.5/23:27 <sup>k</sup>	00:02	8.0	786	274	110	CDAW	-	-	-	-
57/1998.5.6	8210/S11W65	X2.7/07:58	08:29	-	1099	309	190	CDAW	0.32	0.249	0.157	0.502
-	8210	X2.7/07:58	09:32	-1.0	792	328	248	CDAW	-	-	-	-
58/1998.8.24	8307	X1.0(07:58)	-	-	-	-	-	CDAW	-	-	-	-
-	9077	C7.1/6:52	08:30	2.4	395	245	12	SEEDS	-	-	-	-
59/2000.7.14	9077/N22W07	X5.7/10:03	10:54	-	1674	Halo	360	CDAW	0.16	0.219	0.149	0.09
-	9415	C7.7(08:26)	09:30	4.5	403	267	16	CDAW	-	-	-	-
-	9415	C5.3(10:56)	11:18	2.8	511	199	70	CDAW	-	-	-	-
60/2001.4.15	9415/S20W85	X14(13:19)	14:06	-	1199	245	167	CDAW	0.18	0.231	0.196	0.42
-	9415 <sup>c</sup>	-	18:54 <sup>k</sup>	7.5	606	250	10	SEEDS	-	-	-	-
61/2001.4.18	9415/S23W117	west limb	02:30	-	2465	Halo	360	CDAW	0.17	0.293	0.188	0.16
-	9684 <sup>d</sup>	-	13:20	3.1	308	266	6	SEEDS	-	-	-	-
62/2001.11.4	9684/N06W18	X1.0(16:03)	16:35	-	1810	Halo	360	CDAW	0.13	0.195	0.134	0.07
-	9742	<sup>e</sup>	02:06	3.4	800	283	21	CDAW	-	-	-	-
63/2001.12.26	9742/N08W54	M7.1(05:03)	05:30	-	1446	281	>212	CDAW	0.13	0.199	0.208	0.37
-	10069	C4.3/20:33	20:50 <sup>k</sup>	4.7	861	262	131	CDAW/CACT	-	-	-	-
64/2002.8.24	10069/S02W81	X3.1/00:49	01:30	-	Halo	360	1913	CDAW	0.15	0.208	0.138	0.19
-	10486	C9.0/06:13	06:30	5.0	684	110	35	SEEDS <sup>g</sup>	-	-	-	-
-	10486	M5.0/9:20	10:54	0.6	1054	124	147	CDAW	-	-	-	-
65/2003.10.28	10486/S20E02	X17/11:00 <sup>f</sup>	11:30	-	2459	Halo	360	CDAW	0.11	0.201	0.164	0.04

**Table 1** (Continued)

GLE number/date	AR number/loc	FC/onset time <sup>a</sup>	CME time	$\Delta t^b$	CME speed	CPA	AW	Database	Ne/O	Mg/O	Si/O	Fe/O
–	10486	C8.1/16:49	17:36	3.1	567	217	7	CACT/SEEDS <sup>j</sup>	–	–	–	–
66/2003.10.29	10486/S19W09	X10/20:37	20:54	–	2029	Halo	360	CDAW	0.24	0.241	0.172	0.14
–	10486	M1.3/8:39 <sup>g,h</sup>	9:30	8.0	2036	310	326	CDAW/CACT	–	–	–	–
–	10486	<sup>h</sup>	11:30	6.0	826	224	33	CDAW	–	–	–	–
67/2003.11.02	10486/S18W59	X8.3/17:03	17:30	–	2598	Halo	360	CDAW	0.13	0.193	0.119	0.04
–	10720	X2.2/9:06	09:30	0.4	2094	Halo	360	CDAW	–	–	–	–
68/2005.1.17	10720/N14W25	X3.8/9:38 <sup>f</sup>	09:54	–	2547	Halo	360	CDAW	0.18	0.185	0.114	0.04
–	10720	C4.8/3:21	04:06	2.8	503	301	18	CDAW	–	–	–	–
69/2005.1.20	10720/N14W61	X7.1/6:39	06:54	–	3242	Halo	360	CDAW	0.23	0.231	0.162	0.17
–	10930	<sup>i</sup>	20:28	6.2	474	193	50	CDAW	–	–	–	–
70/2006.12.13	10930/S06W23	X3.4/2:17	02:45	–	1774	–	–	CDAW	0.205	0.21	0.20	0.778

<sup>a</sup>Flare class/location, from Gopalswamy et al. 2010b

<sup>b</sup>Delay between the two CMEs are in hours and are calculated from the onset time of CMEs as recorded in the corresponding catalogs

<sup>c</sup>No flares were identified as this is a behind-limb event

<sup>d</sup>No EIT data were available for this event and we did not identify the associated flare

<sup>e</sup>No Solar Geophysical Data on the flare was available. A brightening near AR9742 ~1:30 from the EIT movie at CDAW can be clearly seen

<sup>f</sup>This flare time differs from the Solar Geophysical Data and is from Gopalswamy 2011

<sup>g</sup>We identified this CME by using the C2 movie following a similar approach as used in the SEEDS catalog. The SEEDS catalog did not identify this CME, perhaps due to a bright streamer nearby

<sup>h</sup>The background is too strong for an unambiguous identification of the associated flares

<sup>i</sup>No EIT movie was obtained for this event. No associated flares are identified

<sup>j</sup>This CME is identified as a flow structure (potentially a CME) by the CACT catalog

<sup>k</sup>Indicate the previous day

<sup>l</sup>For the slow solar wind, Ne/O = 0.10, Mg/O = 0.15, Si/O = 0.15, and Fe/O = 0.11

same CMEs that were identified in both SEEDS and CDAW (or other catalogs), the SEEDS catalog often have smaller speeds and widths. This is partly due to the fact that SEEDS often identify CMEs when they are still low.

In Table 1, the 1998 August 24 event had no LASCO data; the 2001 April 18 event is a backside; also in Table 1 event and no flare information were obtained for the preceding CMEs. The remaining 14 GLEs all have at least one preceding CME within 9 hours that has a sky projection speed larger than 300 km/s and are therefore the candidate of the first CME in our “twin CME” scenario. Note for the 2001 November 4 event, the 2001 December 26 event and the 2006 December 13 event, the preceding CMEs do not have associated flares listed. For the 2001 November 4 event, there was no EIT data available so we did not identify the associated flare. For the 2001 December 26 event, no Solar Geophysical Data on the flare was available, but a brightening near AR9742  $\sim$ 1:30 from the EIT movie can be clearly seen. For the 2006 December 13 event no EIT movie was obtained, therefore no associated flares were identified.

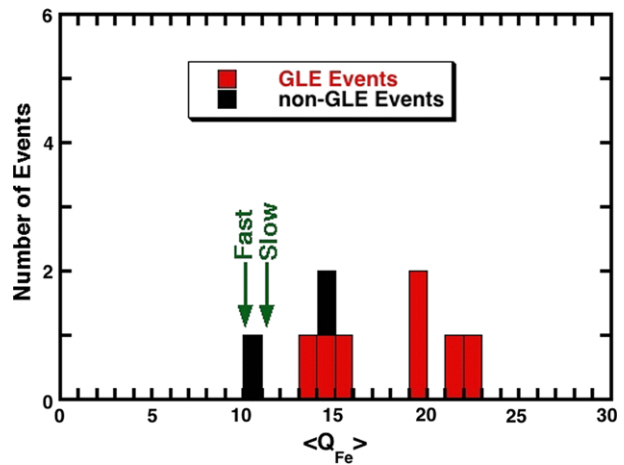
Some of these preceding CMEs are wider than  $60^\circ$ , therefore they were also listed in the study of Gopalswamy et al. (2004). However, many of them are narrow ones and they did not appear in the study of Gopalswamy et al. (2004). They nevertheless are good candidates for our proposed “twin CME” scenario. We made no attempts to estimate the Alfvén speeds in individual events and used a single threshold speed of 300 km/s in all events. We assume shocks can be driven by these CMEs. Because most of these CMEs are narrower and weaker than those CMEs that have type II radio bursts, we did not find clear signatures of type II radio bursts for most of these preceding CMEs. However, for the 2005 January 17 event, where the preceding CME was also fast and wide, a shock is clearly seen from the radio signatures. Perhaps the most important finding of this work is that out of the 14 GLE events in solar cycle 23 where we have the active region information and where CMEs have been observed by SOHO/LASCO, 11 of them have preceding CMEs that originated from the same Active region and have speeds larger than 300 km/s. For the remaining 3 events, preceding CMEs that launched into the same general directions as the primary CMEs are also identified although because of missing flare data, no associated flares were identified. This finding strongly supports our “twin CME” scenario.

Also shown in Table 1 are the ratios of Ne/O, Si/O, Mg/O and Fe/O at 12–30 MeV/nucleon. Although scattered, comparing these to nominal slow solar wind values (von Steiger et al. 2000) listed in the last footnote of Table 1, we do see frequent examples of enhancements that suggest the possible presence of ICME material.<sup>3</sup> Furthermore, we note that the Ne/O value has been used as a proxy for identification of flare material (Reames et al. 1994). Mason et al. (2004) showed that flare material has an average Ne/O ratio of  $0.261 \pm 0.04$ . From the table it is clear that a few of the GLEs have Ne/O ratios comparable to that for flare material, hinting that there could be acceleration of flare material from the first eruption at the 2nd CME shock in these events. As we will discuss in the following, this is possible in our “twin CME” scenario if flare accelerated particles are released on the reconnection field lines as shown in Fig. 1.

Possible evidence for the presence of CME material in large SEP events is provided by measurements of the mean ionic charge state of Fe ( $\langle Q_{\text{Fe}} \rangle$ ) in GLE and other large SEP events. Measurements of a number of large SEP events show that  $\langle Q_{\text{Fe}} \rangle$  varies considerably from event to event, and often increases with energy from values similar to those in the solar wind at  $<1$  MeV/nuc ( $\langle Q_{\text{Fe}} \rangle \sim +10$  to  $+11$ ) to values near  $+20$  at energies  $>10$

<sup>3</sup>We note that heavy ion rich material could also be due to remnant flare material (Mason et al. 1999) or to flare material from the same event.

**Fig. 5** Histograms of the mean ionic charge state of Fe in seven SEP events with a preceding CME and in two events with no preceding CME within the previous 24 hours. Both GLEs and two large non-GLE events are included. Also shown are the mean charge state of Fe in fast and slow solar wind measured by Lepri et al. (2001), and the criterion used by Lepri et al. to identify CME material in the solar wind (the persistent presence of at least 10% of solar wind Fe having  $Q_{\text{Fe}} \geq 16$ )



MeV/nuc (see review by Klecker et al. 2007). There are several possible explanations for the increase in  $\langle Q_{\text{Fe}} \rangle$  with energy, including the presence of highly-ionized suprathermal seed particles due to CME-material as suggested in this paper (see also (Mewaldt et al. 2007)), suprathermal seed particles due to small  $^3\text{He}$ -rich SEP events ((Mason et al. 1999; Tylka et al. 2001; Tylka et al. 2005)) or the mixing of flare and shock accelerated particles (e.g., Cane et al. 2003; Li and Zank 2005). It is also possible that the high charge states are due to stripping during the acceleration process low in the corona (Kovaltsov et al. 2001; Lytova and Kocharov 2005), but this hypothesis is difficult to reconcile with the fact that  $\langle Q_{\text{Fe}} \rangle$  at  $>25$  MeV/nuc is correlated with the Fe/O ratio (Labrador et al. 2005; Mewaldt et al. 2006).

Using SAMPEX data and the geomagnetic technique (Leske et al. 1995; Labrador et al. 2005), we have examined average charge state for 25–90 MeV/nuc Fe for the 1997 Nov 6, the 1998 May 2, the 1998 May 6, the 2000 Jul 14, the 2001 Apr 15, the 2003 Oct 28, and the 2006 Dec 13 GLE events (a total of seven) and two other large, but non-GLE SEP events: the 2001 Sep 24 event and the 2001 Nov 22 event. Figure 5 compares measurements of  $\langle Q_{\text{Fe}} \rangle$  in these events. Also included are charge-state ( $>10$  MeV/nuc) estimates obtained indirectly by fitting SEP abundance variations and time profiles using  $Q/M$ -dependent functions (Cohen et al. 1999; Tylka et al. 2000).

We note that in general GLE events do tend to show higher charge states than the solar wind. This suggests that either the seed population in GLE events are non solar wind-like, consistent with our proposal, or that the acceleration site must have a high density so that the collisional effect cannot be ignored. Note that the mechanism proposed here can apply to large SEP events as well.

#### 4 Discussion and Conclusion

We discuss the “twin-CME scenario” for producing GLEs and extreme SEP events. We propose that when two CMEs occur closely in time and slightly offset in propagation direction, there can be very efficient diffusive shock acceleration at the shock front of the second CME where particles are accelerated to very high energies. Comparing to particle acceleration at a single CME shock, the scenario we propose here has the following distinctive features. First,

the presence of the first CME shock can lead to an enhanced turbulence upstream of the second shock (without significant decay up to  $\sim 9$  hours). Second, magnetic field reconnection between the open magnetic field lines draping the second CME and the closed magnetic field lines enclosing the first CME can leak out driver (mainly ICME in composition) material and flare accelerated ions into the turbulence enhanced upstream of the second CME shock, which then become the seed population for the diffusive shock acceleration process at the second shock. Note that acceleration at the reconnection site effectively pre-accelerates these ions to become the seed particles which have larger speeds than the solar wind and are preferentially accelerated at the second shock. Also note that in our “twin CME” scenario interaction of the two CMEs or their driven shocks is not necessary. The more efficient acceleration than a single shock case is not because of the interactions of the two shocks. Instead, it is due to the presence of strong turbulence and increased suprathermal seed population at the second shock front that is left behind the first shock. In our scenario, we do not require the width of the first CME (and its shock) to be large. Instead, the width of the second CME and its associated shock are deciding factors. The wider it is, the greater the chance it will go through the downstream of the first shock. The time separation of the two CME also affects the maximum energy of the particles accelerated by the second shock. The longer the separation, the smaller the turbulence level due to decay. A 24-hour separation used in Gopalswamy et al. (2004) is perhaps too long, although their average separation turned out to be  $\sim 11$  h. As discussed above, a 9 hour delay is perhaps a rule of thumb for our proposed scenario.

To validate our proposal we have examined all 16 GLE events in solar cycle 23 except the 1998 August 24 event. In all these events, at least one preceding CME was within 9 hours of the primary CME and which has a projection speed  $> 300$  km/s. These preceding CMEs are very capable of driving shocks and provide the pre-accelerated seed population at the second shock through the proposed open-closed field line reconnection. Depending on the magnetic field arrangement of the first shock and the second shock, one may also explain why some of the GLEs are enriched in ICME/flare material but a few are not. Reconnection between open and closed field lines is important in our scenario. Such information can be obtained from the PFSS computed global field as shown in Fig. 3 for the 2003 October 29 event and Fig. 4 for the 2005 January 17 event. From these maps, one can obtain the magnetic polarity of the unipolar open field and the orientation of the closed field line enclosing the driver of the first CME and therefore identify where the reconnection is occurring. In both events, the magnetic field configurations of the ARs are consistent with proposed “twin-CME” scenario. However, we point that these ARs shown in Figs. 3 and 4, by their very nature are very complex and very energetic, and therefore provide other possibilities for extreme particle acceleration. We also note that from a large scale point of view, the magnetic field configuration shown in Fig. 1 and Fig. 2 are both pseudo-streamer like. This kind of configuration is not uncommon due to the global bipolar structure of the outer corona and inner solar wind. We note that although at least 11 out of 14 GLE events we examined agree with our proposed scenario, a control test to verify the “twin CMEs scenario” should be performed. In particular, small gradual SEP events need to be identified and examined (Li et al., 2011). We suggest that these events fail to become large SEP events because there is either no preceding CMEs or in the case there are preceding CMEs, they are weak and slow so a preceding shock may not be formed. Consequently, no efficient acceleration at the second shock can be achieved.

**Acknowledgements** This work is supported in part by NSF ATM-0847719 (CAREER), NASA NNX07AL52A (EpSCoR) and an ORAU Ralph E. Power Junior Faculty Enhancement Award for GL at UAHuntsville. The work at Caltech was supported by NASA grants under grants NNX8A111G and

NNX06AC21G. The authors thank Dr. Nat Gopalswamy and Dr. Nariaki Nitta for organizing the two GLE workshops where this work was largely completed.

## References

- M.J. Aschwanden, Gev particle acceleration in solar flares and ground level enhancement (GLE) events. *Space Sci. Rev.* (2011, submitted)
- W. Axford, The acceleration of galactic cosmic rays: origin of cosmic rays, in *Proceedings of the Symposium*, vol. 1 (Springer, Berlin, 1981), pp. 339–358
- H. Cane, W. Erickson, N. Prestage, Solar flares, type III radio bursts, coronal mass ejections, and energetic particles. *J. Geophys. Res.* **107**(A10), 14–1 (2002). doi:[10.1029/2001JA000320](https://doi.org/10.1029/2001JA000320)
- H. Cane, T. von Roseninge, C. Cohen, R. Mewaldt, Two components in major solar particle events. *Geophys. Res. Lett.* **30**(12), 8017 (2003). doi:[10.1029/2002GL016580](https://doi.org/10.1029/2002GL016580)
- E. Chane, C. Jacobs, B. Van der Holst, S. Poedts, D. Kimpe, On the effect of the initial magnetic polarity and of the background wind on the evolution of CME shocks. *Astron. Astrophys.* **432**, 331–339 (2005). doi:[10.1051/0004-6361:20042005](https://doi.org/10.1051/0004-6361:20042005)
- C. Chen, Y. Wang, C. Shen, P. Ye, J. Zhang, S. Wang, Statistical study of coronal mass ejection source locations. II. Role of active regions in CME production. *J. Geophys. Res.* (2011, submitted). doi:[10.1029/2011JA016844](https://doi.org/10.1029/2011JA016844)
- K.S. Cho, S.C. Bong, Y.H. Kim, Y.J. Moon, M. Dryer, A. Shanmugaraju, J. Lee, Y.D. Park, Low coronal observations of metric type II associated CMEs by MLSO coronameters. *Astron. Astrophys.* **491**, 873–882 (2008). doi:[10.1051/0004-6361:20079013](https://doi.org/10.1051/0004-6361:20079013)
- E. Cliver, S. Kahler, D. Reames, Coronal shocks and solar energetic proton events. *Astrophys. J.* **605**(2, Part 1), 902–910 (2004)
- C.M.S. Cohen, A.C. Cummings, R.A. Leske, R.A. Mewaldt, E.C. Stone, B.L. Dougherty, M.E. Wiedenbeck, E.R. Christian, T.T. von Roseninge, Inferred charge states of high energy solar particles from the solar isotope spectrometer on ace. *Geophys. Res. Lett.* **26**, 149–152 (1999)
- C. Cohen, R. Mewaldt, A. Cummings, R. Leske, E. Stone, T. von Roseninge, M. Wiedenbeck, Variability of spectra in large solar energetic particle events, in *Energy Release and Particle Acceleration in the Solar Atmosphere—Flares and Related Phenomena*, ed. by B. Dennis, T. Kosugi, R. Lin. *Advances in Space Research*, vol. 32 (Pergamon-Elsevier, Oxford, 2003), pp. 2649–2654. doi:[10.1016/S2073-1177\(03\)00901-3](https://doi.org/10.1016/S2073-1177(03)00901-3)
- M. Desai, G. Mason, J. Dwyer, J. Mazur, R. Gold, S. Krimigis, C. Smith, R. Skoug, Evidence for a suprathermal seed population of heavy ions accelerated by interplanetary shocks near 1 AU. *Astrophys. J.* **588**(2, Part 1), 1149–1162 (2003)
- M. Desai, G. Mason, M. Wiedenbeck, C. Cohen, J. Mazur, J. Dwyer, R. Gold, S. Krimigis, Q. Hu, C. Smith, R. Skoug, Spectral properties of heavy ions associated with the passage of interplanetary shocks at 1 AU. *Astrophys. J.* **611**(2, Part 1), 1156–1174 (2004)
- L. Drury, An introduction to the theory of diffusive shock acceleration of energetic particles in tenuous plasmas. *Rep. Prog. Phys.* **46**(8), 973–1027 (1983)
- R.M. Evans, M.M. Opher, W.B. Manchester, T.I. Gombosi, Alfvén profile in the lower corona: implications for shock formation. *Astrophys. J.* **687**, 1355–1362 (2008)
- N. Gopalswamy, A. Lara, M.L. Kaiser, J.-L. Bougeret, Near-Sun and near-Earth manifestations of solar eruptions. *J. Geophys. Res.* **106**, 25261–25278 (2001)
- N. Gopalswamy, S. Yashiro, S. Krucker, G. Stenborg, R. Howard, Intensity variation of large solar energetic particle events associated with coronal mass ejections. *J. Geophys. Res.* **109**(A12) (2004). doi:[10.1029/2004JA010602](https://doi.org/10.1029/2004JA010602)
- N. Gopalswamy, E. Aguilar-Rodríguez, S. Yashiro, S. Nunes, M. Kaiser, R. Howard, Type II radio bursts and energetic solar eruptions. *J. Geophys. Res.* **110**(A12), 12–07 (2005). doi:[10.1029/2005JA011158](https://doi.org/10.1029/2005JA011158)
- N. Gopalswamy, W.T. Thompson, J.M. Davila, M.L. Kaiser, S. Yashiro, P. Mäkelä, G. Michalek, J.L. Bougeret, R.A. Howard, Relation between type II bursts and cmes inferred from stereo observations. *Sol. Phys.* **259**(1–2), 227–254 (2009). doi:[10.1007/s11207-009-9382-1](https://doi.org/10.1007/s11207-009-9382-1)
- N. Gopalswamy, H. Xie, P. Makela, S. Akiyama, S. Yashiro, M.L. Kaiser, R.A. Howard, J.L. Bougeret, Interplanetary shocks lacking type II radio bursts. *Astrophys. J.* **710**(2), 1111–1126 (2010a)
- N. Gopalswamy, H. Xie, S. Akiyama, P. Makela, I.G. Usoskin, Properties of Ground level enhancement events of solar cycle 23. *Ind. J. Space and Radio Phys.* **39**, 240–248 (2010b) doi:[10.1088/0004-6256/710/2/1111](https://doi.org/10.1088/0004-6256/710/2/1111)
- N. Gopalswamy, H. Xie, S. Yashiro, S. Akiyama, P. Mäkelä, I.G. Usoskin, Properties of Ground level enhancement events and the associated solar eruptions during solar cycle 23. *Space Sci. Rev.* (2011, submitted)

- G. Ho, G. Mason, E. Roelof, R. Gold, J. Mazur, Peak proton intensities and composition variations of heavy ions during large solar energetic particle events: Uleis observations, in *Heliosphere at Solar Maximum*, ed. by M. Potgieter, B. Heber, H. Fichtner, R. Marsden. Advances in Space Research, vol. 32 (Pergamon/Elsevier, Oxford, 2003), pp. 561–566. doi:[10.1016/S0273-1177\(03\)00355-7](https://doi.org/10.1016/S0273-1177(03)00355-7)
- F.M. Ipavich, A.B. Galvin, G. Gloeckler, D. Dovestadt, B. Klecker, Solar wind Fe and CNO measurements in high-speed flows. *J. Geophys. Res.* **91**, 4133–4141 (1986)
- S.W. Kahler, Radio burst characteristics of solar proton flares. *Astrophys. J.* **261**, 710–719 (1982)
- S.W. Kahler, Coronal mass ejections and solar energetic particle events, in *High Energy Solar Physics: AIP Conference Proceedings*, vol. 374 (1996), pp. 61–77
- S.W. Kahler, D.V. Reames, J.T. Burkepile, A role for ambient energetic particle intensities in shock acceleration of solar energetic particles, in *High Energy Solar Physics: Anticipating HESSI*. ASP Conf., vol. 206 (2000), p. 468
- B. Klecker, E. Moebius, M.A. Popecki, Ionic charge states of solar energetic particles: a clue to the source. *Space Sci. Rev.* **130**(1–4), 273–282 (2007). doi:[10.1007/s11214-007-9207-1](https://doi.org/10.1007/s11214-007-9207-1)
- G.A. Kovaltsov, A.F. Barghouty, L. Kocharov, V.M. Ostryakov, J. Torsti, Charge-equilibration of Fe ions accelerated in a hot plasma. *Astron. Astrophys.* **375**, 1075–1081 (2001)
- A.W. Labrador, L.R. A, R.A. Mewaldt, E.C. Stone, T.T. von Roseninge, High energy ionic charge state composition in the October/November 2003 and January 20, 2005 Sep events, in *Proceedings of the 29th ICRC*, vol. 1 (2005), pp. 99–102
- S.T. Lepri, T.H. Zurbuchen, L.A. Fisk, I.G. Richardson, H.V. Cane, G. Gloeckler, Iron charge distribution as an identifier of interplanetary coronal mass ejections. *J. Geophys. Res.* **106**, 29231–29238 (2001)
- R.A. Leske, J.R. Cummings, R.A. Mewaldt, E.C. Stone, T.T. von Roseninge, Measurements of the ionic charge states of solar energetic particles using the geomagnetic-field. *Astrophys. J.* **452**(2, Part 2), 149–152 (1995)
- G. Li, Diffusive shock acceleration and ground level events. *Space Sci. Rev.* (2011, submitted)
- G. Li, R.A. Mewaldt, Can multiple shocks trigger ground level events, in *Proceedings of the 31st ICRC SH* (2009), p. 1362
- G. Li, G.P. Zank, Multiple CMEs and large gradual SEP events, in *29th ICRC Proceedings*, vol. 1 (2005), p. 173
- G. Li, G. Zank, W. Rice, Energetic particle acceleration and transport at coronal mass ejection-driven shocks. *J. Geophys. Res.* **108**(A2), 10–1 (2003). doi:[10.1029/2002JA009666](https://doi.org/10.1029/2002JA009666)
- J. Lin, S. Mancuso, A. Vourlidas, Theoretical investigation of the onsets of type II radio bursts during solar eruptions. *Astrophys. J.* **649**, 1110 (2006)
- G. Li, L. Ding, Y. Jiang, L. Zhao, The “twin-CME” scenario and large Solar Energetic Particle events in Solar Cycle 23. *J. Geophys. Res.* (2011, submitted)
- R.P. Lin et al., The Reuven Ramaty high-energy solar spectroscopic imager (Rhessi). *Sol. Phys.* **210**, 3 (2002)
- N. Lugaz, W.B. Manchester, I. Roussev, G. Toth, T.I. Gombosi, Numerical investigation of the homologous coronal mass ejection events from active region 9236. *Astrophys. J.* **659**, 788–800 (2007a)
- M. Lytova, L. Kocharov, Charge states of energetic solar ions from coronal shock acceleration. *Astrophys. J.* **620**, 55–58 (2005)
- G.M. Mason, J.E. Mazur, J.R. Dwyer, 3He enhancements in large solar energetic particle events. *Astrophys. J.* **525**, 133–136 (1999)
- G. Mason, J. Mazur, J. Dwyer, J. Jokipii, R. Gold, S. Krimigis, Abundances of heavy and ultraheavy ions in He-3-rich solar flares. *Astrophys. J.* **606**(1, Part 1), 555–564 (2004)
- R. Mewaldt, C. Cohen, A. Labrador, R. Leske, G. Mason, M. Desai, M. Looper, J. Mazur, R. Selesnick, D. Haggerty, Proton, helium, and electron spectra during the large solar particle events of October–November 2003. *J. Geophys. Res.* **110**(A9), (2005). doi:[10.1029/2005JA011038](https://doi.org/10.1029/2005JA011038)
- R. Mewaldt, C. Cohen, G. Mason, The source material for large solar energetic particle events, in *Solar Eruptions and Energetic Particles*, ed. by N. Gopalswamy et al. Geophysical Monograph Series, vol. 165, (2006), p. 115
- R.A. Mewaldt, C.M.S. Cohen, G.M. Mason, A.C. Cummings, M.I. Desai, R.A. Leske, J. Raines, E.C. Stone, M.E. Wiedenbeck, T.T. von Roseninge, T.H. Zurbuchen, On the differences in composition between solar energetic particles and solar wind. *Space Sci. Rev.* **130**(1–4), 207–219 (2007). doi:[10.1007/s11214-007-9187-1](https://doi.org/10.1007/s11214-007-9187-1)
- R. Mewaldt, M.D. Looper, C.M.S. Cohen, D.K. Haggerty, A.W. Labrador, R.A. Leske, G.M. Mason, J.E. Mazur, Spectra and properties of ground-level events during solar cycle 23, in *31st International Cosmic Ray Conference Proceedings*, vol. 1 (2009)
- R.A. Mewaldt, L.M. D., C.M.S. Cohen, D.K. Haggerty, A.W. Labrador, R.A. Leske, G.M. Mason, J.E. Mazur, T.T. von Roseninge, Energy spectra, composition, and other properties of ground-level events during solar cycle 23. *Space Sci. Rev.* (2011, submitted)

- H. Moraal, K.G. McCracken, The time structure of ground level enhancements in solar cycle 23. *Space Sci. Rev.* (2011). doi:[10.1007/s11214-011-9742-7](https://doi.org/10.1007/s11214-011-9742-7)
- N.V. Nitta, Y. Liu, M.L. DeRosa, R.W. Nightingale, Active regions associated with ground-level events. *Space Sci. Rev.* (2011, submitted)
- N.V. Nitta, H.S. Hudson, Recurrent FLARE/CME events from an emerging flux region. *Geophys. Res. Lett.* **28**, 3801–3804 (2001)
- D.V. Reames, J.P. Meyer, T.T. von Roseninge, Energetic-particle abundances in impulsive solar flare events. *Astrophys. J. Suppl. Ser.* **90**, 649–667 (1994)
- D.V. Reames, Solar release times of energetic particles in ground-level events. *Astrophys. J.* **693**(1), 812–821 (2009). doi:[10.1088/0004-637X/693/1/812](https://doi.org/10.1088/0004-637X/693/1/812)
- D. Reames, Coronal abundances determined from energetic particles. *Adv. Space Res.* **15**, 41–51 (1995)
- D. Reames, Particle acceleration at the sun and in the heliosphere. *Space Sci. Rev.* **90**, 413–491 (1999)
- M.J. Reiner, M.L. Kaiser, N. Gopalswamy, H. Aurass, G. Mann, A. Vourlidis, M. Maksimovic, Statistical analysis of coronal shock dynamics implied by radio and white-light observations. *J. Geophys. Res.* **106**, 25279 (2001)
- W. Rice, G. Zank, G. Li, Particle acceleration and coronal mass ejection driven shocks: shocks of arbitrary strength. *J. Geophys. Res.* **108**(A10), 5–1 (2003). doi:[10.1029/2002JA009756](https://doi.org/10.1029/2002JA009756)
- I. Richardson, H. Cane, The fraction of interplanetary coronal mass ejections that are magnetic clouds: evidence for a solar cycle variation. *Geophys. Res. Lett.* **31**(18), (2004). doi:[10.1029/2004GL020958](https://doi.org/10.1029/2004GL020958)
- K. Schrijver, M.L. DeRosa, Photospheric and heliospheric magnetic fields. *Sol. Phys.* **212**, 165–200 (2003)
- A.Y. Shih, R.P. Lin, D.M. Smith, Rhesi observations of the proportional acceleration of relativistic  $> 0.3$  MeV electrons and  $> 30$  MeV protons in solar flares. *Astrophys. J. Lett.* **698**(2), 152–157 (2009). doi:[10.1088/0004-637X/698/2/L152](https://doi.org/10.1088/0004-637X/698/2/L152)
- A.J. Tylka, P.R. Boberg, J.H. Adams, L.P. Beahm, W.F. Dietrich, T. Kleis, The mean ionic charge state of solar energetic Fe ions above 200 MeV per nucleon. *Astrophys. J.* **444**, 109–113 (1995)
- A.J. Tylka, P.R. Boberg, R.E. McGuires, C.K. Ng, D.V. Reames, Temporal evolution in the spectra of gradual solar energetic particle events. 2000 Symposium, in *AIP Conference Proceedings*, vol. 528, (2000), pp. 147–152
- A.J. Tylka, C.M.S. Cohen, W.F. Dietrich, C.G. MacLennan, R.E. McGuires, C.K. Ng, D.V. Reames, Evidence for remnant flares suprathermal in the source population of solar energetic particles in the 2000 Bastille day event. *Astrophys. J.* **558**, 59–63 (2001)
- A.J. Tylka, C.M.S. Cohen, W.F. Dietrich, S. Krucker, R.E. McGuires, R.A. Mewaldt, C.K. Ng, D.V. Reames, G.H. Share, Onsets and release times in solar particle events, in *28th ICRC Proceedings*, vol. 1 (2003)
- A. Tylka, C. Cohen, W. Dietrich, M. Lee, C. MacLennan, R. Mewaldt, C. Ng, D. Reames, Shock geometry, seed populations, and the origin of variable elemental composition at high energies in large gradual solar particle events. *Astrophys. J.* **625**(1, Part 1), 474–495 (2005)
- R. von Steiger, N.A. Schwadron, L.A. Fisk, J. Geiss, G. Gloeckler, S. Hefti, B. Wilken, R.F. Wimmer-Schweingruber, T.H. Zurbuchen, Composition of quasi-stationary solar wind flows from Ulysses/solar wind ion composition spectrometer. *J. Geophys. Res.* **105**, 27217–27238 (2000)
- A. Wang, S.T. Wu, N. Gopalswamy, Magnetohydrodynamic analysis of the January 20, 2001, CME-CME interaction effect. *Geophys. Monogr.* **156**, 185 (2005)
- G. Zank, W. Rice, C. Wu, Particle acceleration and coronal mass ejection driven shocks: a theoretical model. *J. Geophys. Res.* **105**(A11), 25079–25095 (2000)
- T.V. Zaqarashvili, R. Oliver, J.L. Ballester, Spectral line width decrease in the solar corona: resonant energy conversion from Alfvén to acoustic waves. *Astron. Astrophys.* **456**, 13–16 (2006)
- T.H. Zurbuchen, L.A. Fisk, G. Gloeckler, R. von Steiger, The solar wind composition throughout the solar cycle: a continuum of dynamic states. *Geophys. Res. Lett.* **29**, 1352–1010292001013946 (2002)